



Supplement of

Roughness of fracture surfaces in numerical models and laboratory experiments

Steffen Abe and Hagen Deckert

Correspondence to: Steffen Abe (s.abe@igem-energie.de)

The copyright of individual parts of the supplement might differ from the article licence.



Figure S1: Fragments of a limestone sample after a triaxial deformation experiment.

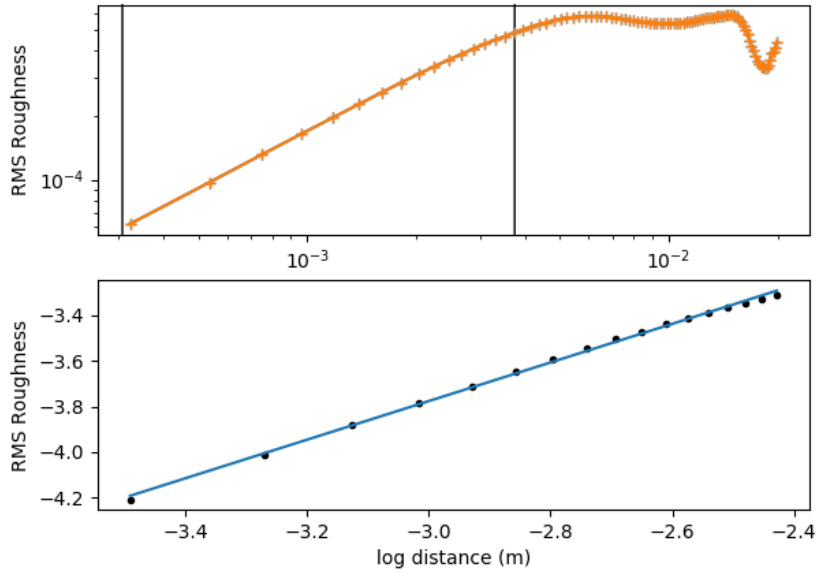


Figure S2: Height-height correlation function for the Limestone sample. Top: Full distance range, bottom: range used for fitting a linear relation and calculation of Hurst-exponent.

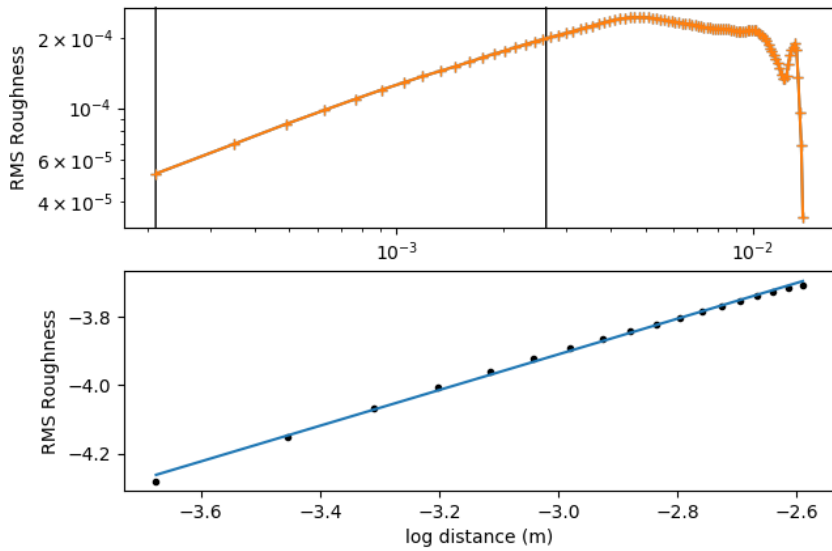


Figure S3: Height-height correlation function for the Sandstone sample. Top: Full distance range, bottom: range used for fitting a linear relation and calculation of Hurst-exponent

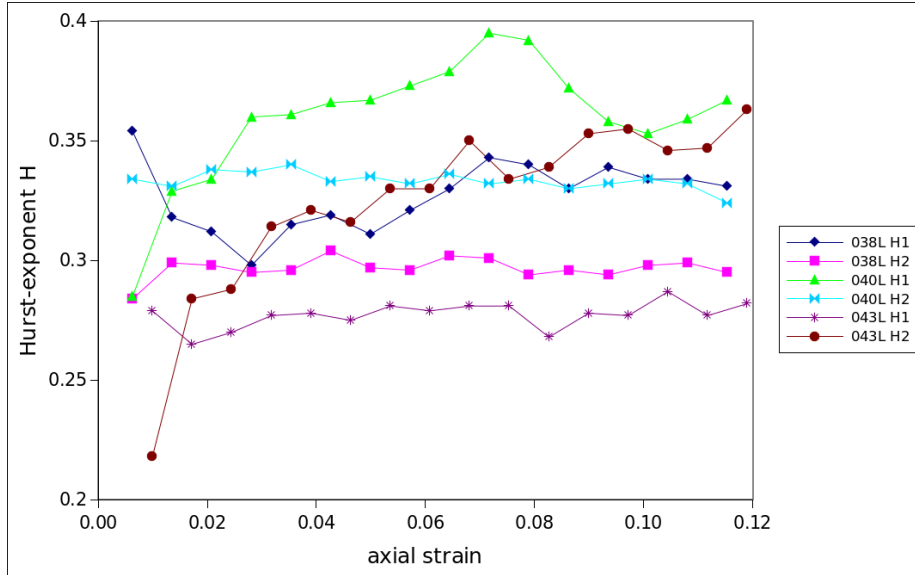


Figure S4: Hurst exponent of fracture surfaces vs. axial strain of deformed sample for 6 surfaces from 3 numerical models. In the legend, the 1st part of the description (038L) is the model ID, the 2nd part (H1, H2) distinguishes between the two surfaces of the fracture.

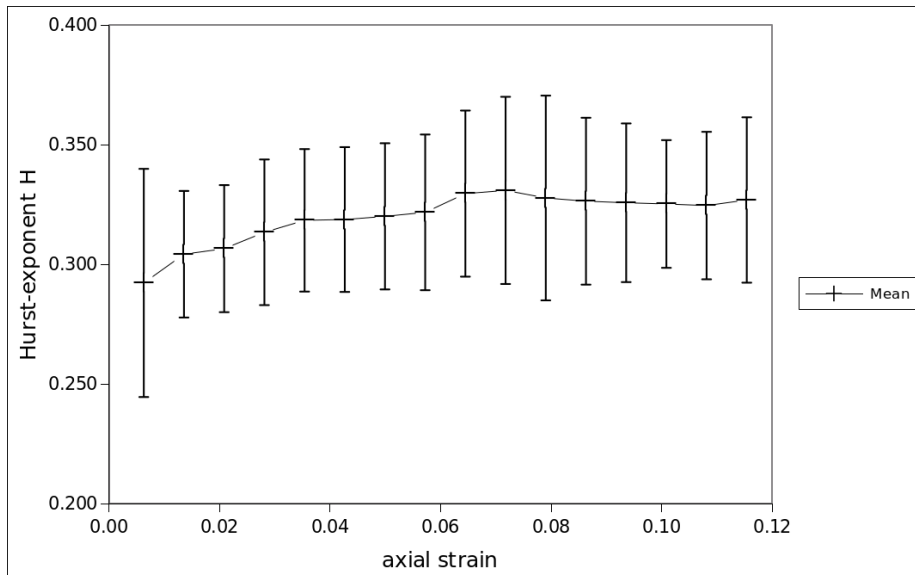


Figure S5: Average of the Hurst exponents of the 6 surfaces shown in Fig. ?? vs. model strain. Error bars show standard deviation

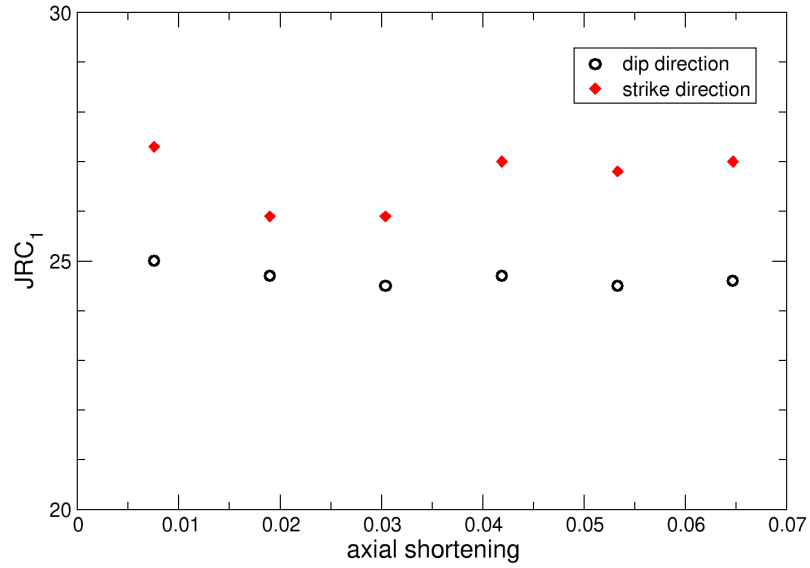


Figure S6: Evolution of the JRC with increasing shear offset of the surfaces. Data points are averages of the two surfaces of the same shear fracture.

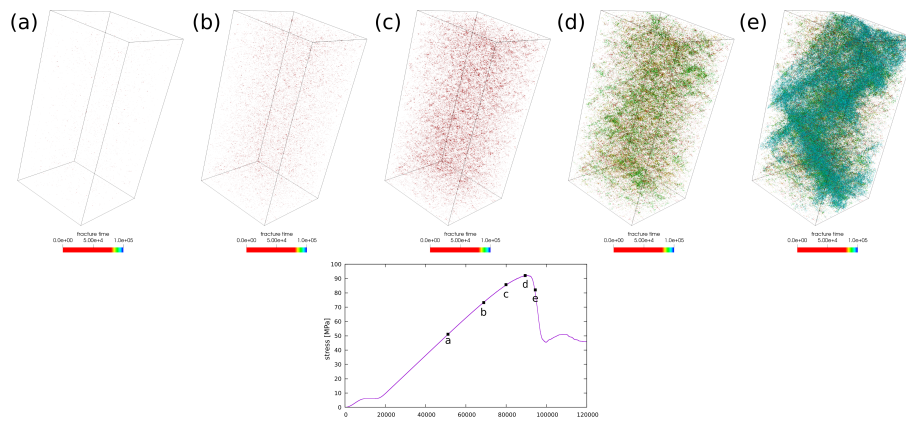


Figure S7: Evolution of micro-crack distribution in model with biaxial loading ($\sigma_2 = \sigma_3 = 6\text{MPa}$). Timing of the snapshots is shown on a plot of axial stress over time below the snapshots. Individual micro-cracks are colored by failure time.

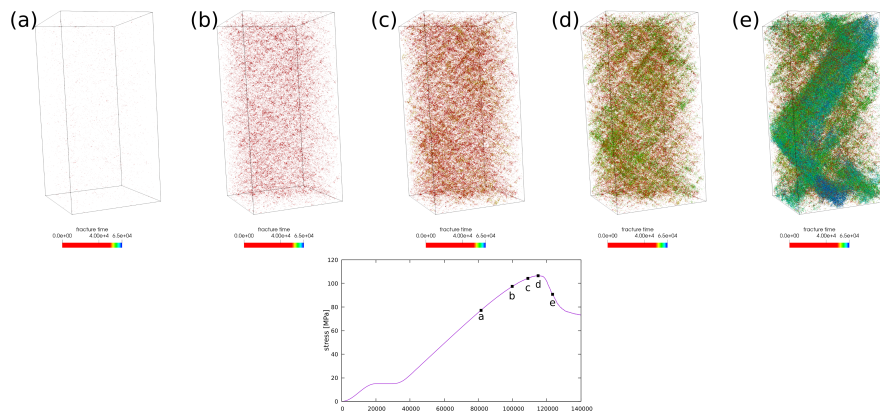


Figure S8: Evolution of micro-crack distribution in model with triaxial loading ($\sigma_2 = 15\text{MPa}$, $\sigma_3 = 6\text{MPa}$). Timing of the snapshots is shown on a plot of axial stress over time below the snapshots. Individual micro-cracks are colored by failure time.